catalysts

MDPI

Article

Novel Functionality of Lithium-Impregnated Titania as Nanocatalyst

Indu Ambat [1,*], Varsha Srivastava [1], Esa Haapaniemi [2] and Mika Sillanpää [1]

[1] Department of Green Chemistry, LUT University, Sammonkatu 12, FI-50130 Mikkeli, Finland; varsha.srivastava@lut.fi (V.S.); mika.sillanpaa@lut.fi (M.S.)
[2] Department of Organic Chemistry, University of Jyväskylä, 40014 Jyväskylän yliopisto, Finland; esa.a.haapaniemi@jyu.fi
* Correspondence: indu.ambat@outlook.com

Received: 20 October 2019; Accepted: 7 November 2019; Published: 9 November 2019

Abstract: The present work incorporates the synthesis of a multifunctional catalyst for the transesterification of waste cooking oil (WCO) to biodiesel and recovery of rare earth elements (REEs). For this purpose, TiO_2 nanoparticles and TiO_2 doped with lithium ions were prepared. The influence of lithium ions on the catalytic performance of TiO_2 was attained by impregnation of the different molar ratios of lithium hydroxide to bare TiO_2. Then each catalyst was screened for catalytic conversion of WCO to fatty acid methyl ester (FAME) and also for REEs recovery. All synthesized materials were characterized using scanning electron microscopy (SEM), X-ray diffraction (XRD), Transmission electron microscopy (TEM), Brunauer–Emmett–Teller (BET) analysis, and Hammett indicator for the basicity test. The obtained biodiesel was characterized by gas chromatography with mass spectrometry (GC-MS), ^{1}H, and ^{13}C nuclear magnetic resonance (NMR). Moreover, the physical parameters of the synthesized biodiesel were also determined. The REEs recovery efficiency of synthesized nanomaterials was investigated, and the percentage of REEs removal was determined by inductively-coupled plasma optical emission spectroscopy (ICP-OES).

Keywords: biodiesel; rare earth elements; TiO_2; nanocatalyst; waste cooking oil

1. Introduction

The rise in population results in the diminution of fossil fuels, and environmental pollution leads to the requirement for an alternative fuel [1,2]. The advancement in technology and the growing population also result in the accumulation of waste containing rare earth elements (REEs) [3–5]. REEs are toxic to living entities and have an inevitable role in various areas such as electronics, batteries, optics, and laser technology. Therefore, the recycling of REEs and the replacement of conventional fuels with renewable energy are significant parts of sustainability, to meet the increasing demand for rare earth elements and fuels, and to reduce the health problems and pollution due to REEs deposition and fossil fuel consumption respectively [1–6].

In recent days, conventional fuels can be replaced by biodiesel produced from fats/oils by the transesterification method. The availability, sustainability, and renewability make biodiesel an economical and eco-friendly source of energy [7–10]. The waste cooking oil was used for the production of high-quality biodiesel due to its cost-effective nature and did not compete with the food market [1,2,8]. The conventional techniques used for REEs recovery from aqueous solutions were precipitation, solvent extraction, adsorption, and ion exchange methods. All these processes, except adsorption, require a considerable cost of operation and non-environmentally-friendly by-products [5,11,12]. Based on previously-reported studies, materials constructed on cellulose, silica, chitosan, carbon, and calcium were widely used for the recovery of rare earth metals [4,13,14].

Presently, nanocatalysts show a vital part in the conversion of different sources such as edible/non-edible oil, fat/waste cooking oil, and algal oil to biodiesel [5,8,10,15,16]. Nanocatalysts were highly recommended for the transesterification process because of their increased catalytic activity, and their economical and environmentally friendly nature [5,8,17]. In addition, the earlier reported studies specified that nanomaterials also performed a significant role in the recovery of REEs from wastewater sources due to their improved surface area, reusability, and lower difficulty in mass transfer [1,3,8,12].

The main objective of the current work was to synthesize a multipurpose catalyst, which would be able to perform biodiesel production and recovery of REEs in an efficient way. The work was focused on the synthesis of lithium-impregnated TiO_2 in which the loading effect on catalytic performance was observed by impregnating different concentrations of lithium to titania. Moreover, the production of biodiesel and recovery of REEs using lithium-doped TiO_2 has not been investigated. The characterization of lithium-doped titanium dioxide was done using SEM, XRD, TEM, Brunauer–Emmett–Teller (BET) analysis, and Hammett indicators for the basicity test. The percentage recovery of REEs and biodiesel production from waste cooking oil (WCO) using lithium-doped TiO_2 was analyzed. The fatty acid methyl ester (FAME) composition and percentage conversion of WCO to FAME were examined by gas chromatography with mass spectrometry (GC-MS), ^{1}H, and ^{13}C NMR techniques. The properties of the obtained biodiesel were analyzed. The efficiency of REEs adsorption using nanomaterials was investigated with the help of inductively coupled plasma optical emission spectroscopy (ICP-OES).

2. Result and Discussion

2.1. Characterization of Nanocatalysts

Figure 1 shows the XRD pattern of TiO_2 and lithium-doped TiO_2. The unmodified TiO_2 X-ray diffraction spectra show an excellent match to standard reference code ICDD: 98-015-4607, anatase titania [2]. Briefly, the XRD peaks of the TiO_2-0.25Li nanocatalyst provided a constant harmony to reference standard code ICSD: 96947, ICDD: 98-009-6947, lithium titanium oxide (0.03/1/2) whereas TiO2-0.5Li and TiO_2-0.75Li showed a good match to standard reference code ICSD: 84713, ICDD: 98-008-4713, lithium titanium oxide (0.74/3/6). The crystallographic factors of the prepared catalysts are summarized in Table 1.

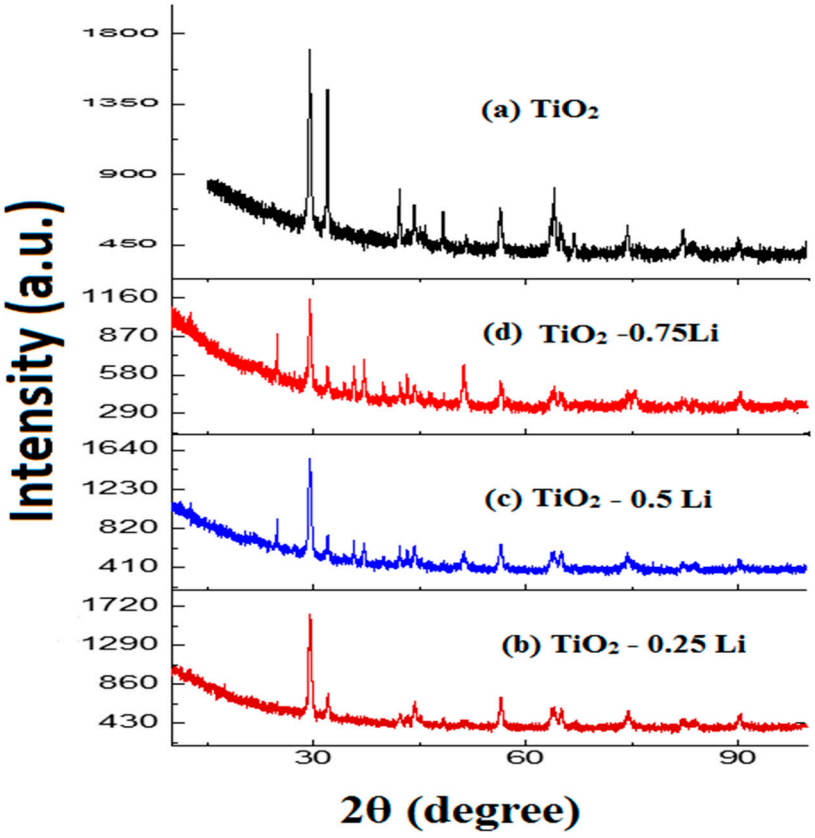

Figure 1. XRD pattern of unmodified TiO_2 and lithium-impregnated TiO_2.

Table 1. The crystallographic parameters of synthesized catalysts.

Catalyst	Crystal Structure	a	b	c	A	β	γ	Density
		(nm)	(nm)	(nm)				(g/cm^3)
TiO_2	Tetragonal	0.38	0.38	0.94	90	90	90	3.93
TiO_2-0.25Li	Tetragonal	0.38	0.38	0.95	90	90	90	3.89
TiO_2-0.5Li	Monoclinic	14.12	2.95	4.94	90	92.7	90	3.96
TiO_2-0.75Li	Monoclinic	14.12	2.95	4.94	90	92.7	90	3.96

SEM was performed to study the surface morphology of the synthesized nanocatalysts. The SEM images of bare TiO_2 and lithium-impregnated TiO_2 are represented in Figure 2. The particles in bare TiO_2 had fluffier morphology and evenly distributed nature. The SEM images of lithium-loaded catalysts showed a significant alteration in morphology compared to the unmodified TiO_2 catalyst. The agglomeration of particles was visible in lithium-ion-inserted TiO_2 surface morphology, possibly due to the addition of lithium particles on the surface of TiO_2. Furthermore, the doping of lithium particles on the surface of TiO_2 resulted in a cluster of particles and a reduction in sponginess. The agglomeration of particles rose with an increase in lithium-ion impregnation.

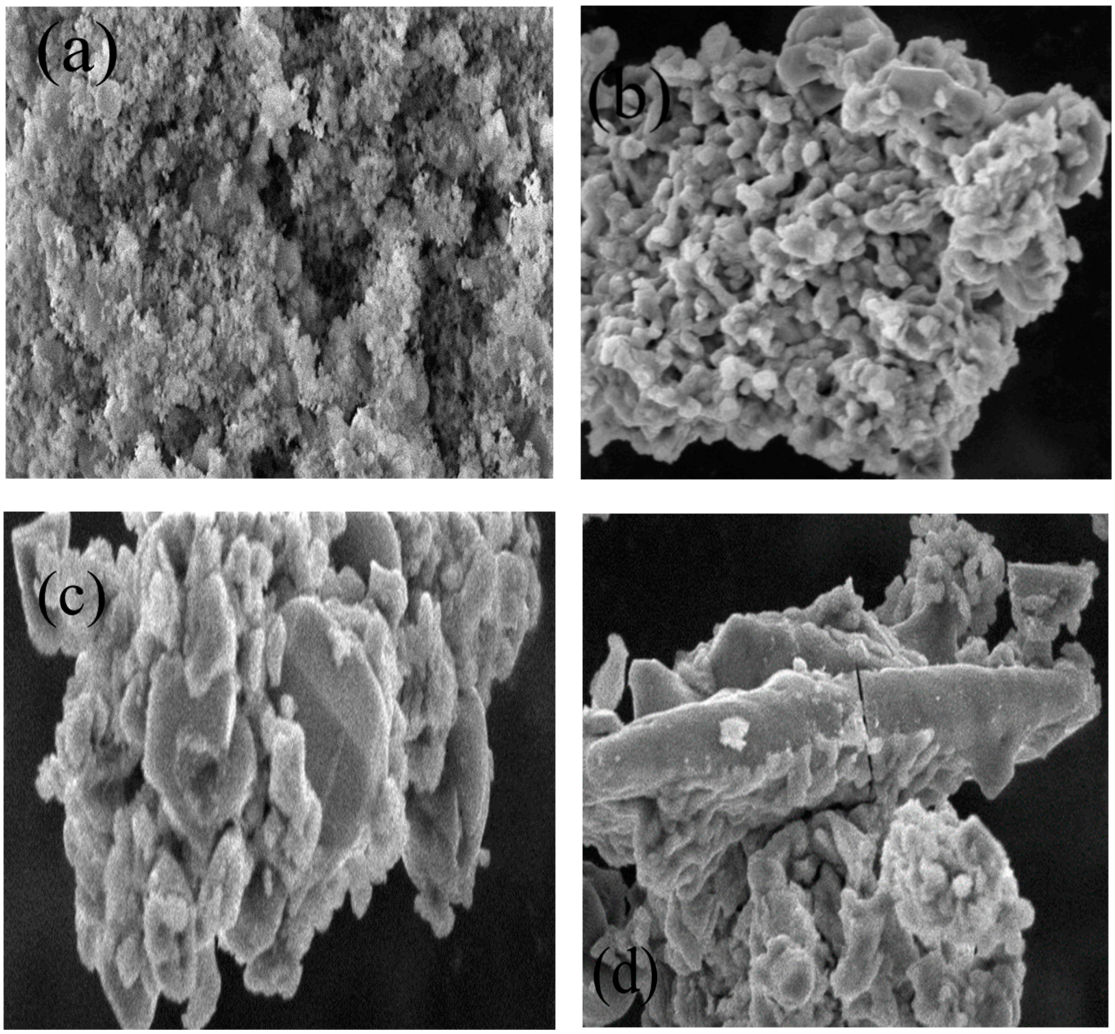

Figure 2. SEM images of (**a**) TiO_2, (**b**) TiO_2-0.25Li, (**c**) TiO_2-0.5Li, and (**d**) TiO_2-0.75Li.

The TEM images of TiO_2 and lithium-doped TiO_2 are depicted in Figure 3. The bare TiO_2 and lithium impregnated TiO_2 had a particle size of 25–48 nm and 30–198 nm correspondingly. TEM results confirmed the catalyst particle size. Figure 3b–d denotes that the agglomeration of particles in the catalyst and drop in the porosity of the catalyst rose with increased concentration of lithium ions. Moreover, the TEM results were in good fit with the SEM images.

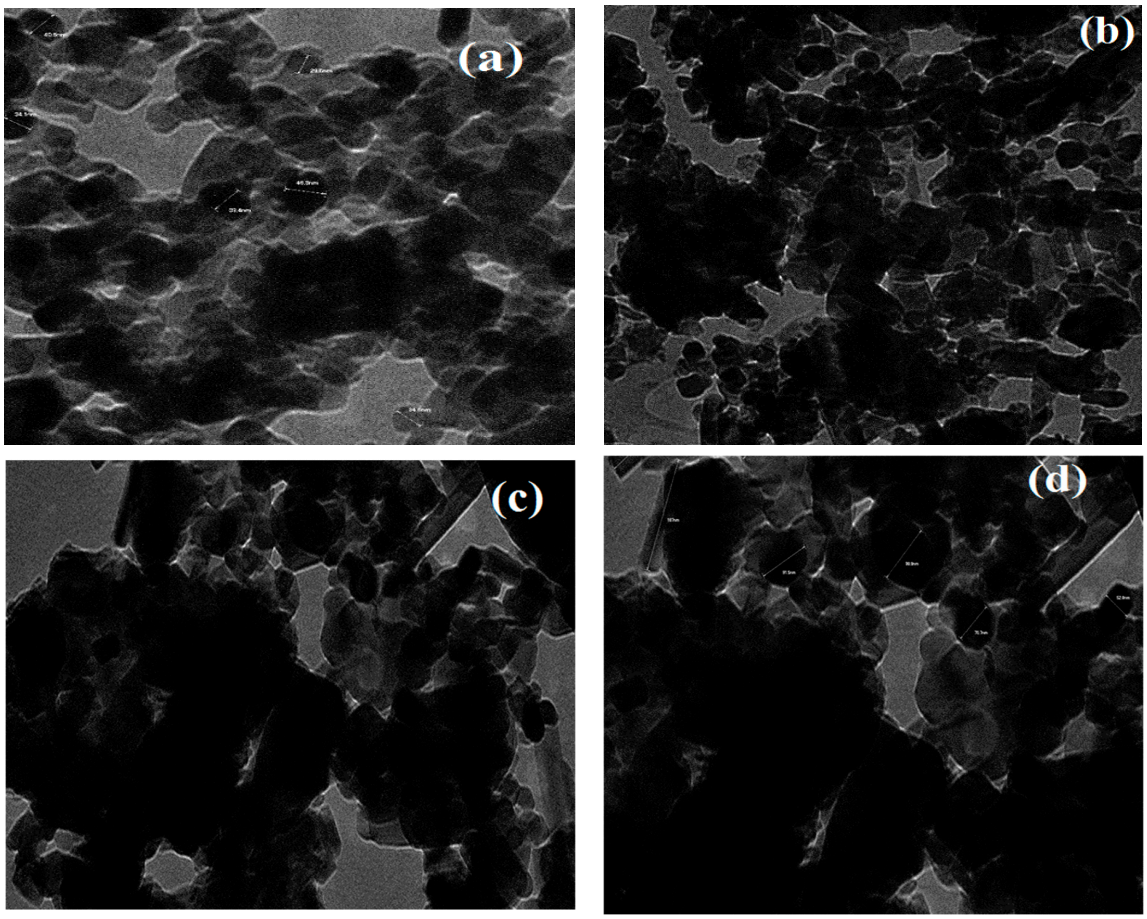

Figure 3. TEM images of (**a**) TiO_2, (**b**) TiO_2-0.25Li, (**c**) TiO_2-0.5Li, and (**d**) TiO_2-0.75Li.

The nitrogen adsorption–desorption measurements were performed to determine the surface area, pore volume, and pore size of TiO_2 and lithium-doped TiO_2 catalysts. The BET analysis of different catalysts is shown in Table 2. The drop in surface area and pore volume was observed after the impregnation of lithium ions to TiO_2. The reduction in porosity in lithium-doped TiO_2 was maybe due to the addition of lithium ions in pores. The nanomaterial showed significant catalytic activity with an increase in impregnation of lithium ions; conversely, a drop in surface area and porosity. The rise in catalytic activity was possibly due to the basic strength of catalytic sites in the nanomaterial, which enhances the conversion of WCO to FAME [16,17]. The BET adsorption–desorption isotherm plot for the synthesized catalysts are given in Figure 4. The nature of the isotherm specifies the presence of mesoporous materials.

Table 2. Brunauer–Emmett–Teller (BET) results of various catalysts.

Catalyst	BET Surface Area (m^2g^{-1})	Pore Volume (cm^3g^{-1})	Pore Size (nm)
TiO_2	37.6	0.060	65.7
TiO_2:0.25Li	29.2	0.052	69.2
TiO_2:0.5Li	19.8	0.035	75.2
TiO_2:0.75LiOH	14.2	0.028	71.9

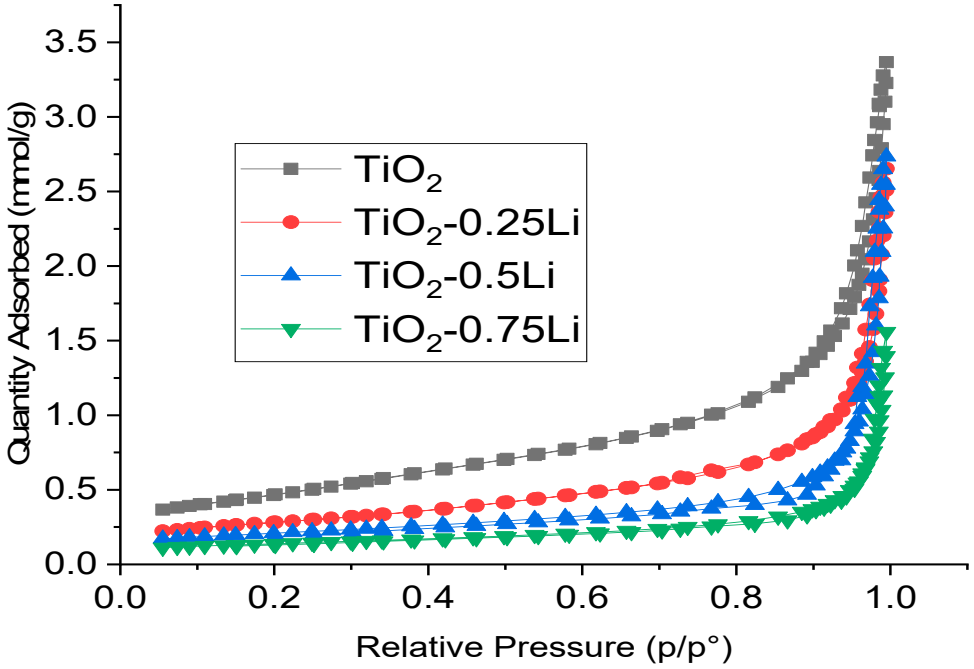

Figure 4. BET isotherm plots of the synthesized catalysts.

2.2. Selection of Catalyst for Biodiesel Production

The best catalyst choice was determined by conducting the transesterification of WCO using a series of catalysts like TiO_2, and TiO_2-LiOH (1:0.25, 1:0.5, and 1:0.75 molar ratios). The reaction was carried out using oil to methanol in a 1:6 molar ratio with 3 wt% of each nanocatalyst at 65 °C for 120 min. The catalytic efficiency of each catalyst and properties of obtained FAME are shown in Table 3. Besides, reaction conditions for the selected catalyst were optimized to achieve a high yield of fatty acid methyl esters (FAME).

Table 3. The catalytic performance of various catalyst for transesterification of waste cooking oil (WCO).

Catalyst	Molar Ratio	Total Basicity (mmol g^{-1})	BET Surface Area (m^2g^{-1})	FAME Conversion (C%)	Density at 15 °C (kg/m^3)	Kinematic Viscosity at 40 °C (mm^2/s)	Flash Point (°C)
TiO_2	-	0.1	37.6	No reaction	-	-	-
TiO_2:LiOH	1:0.25	1.1	29.2	66.2	860.7	3.1	139
TiO_2:LiOH	1:0.5	1.71	19.8	92.1	879.4	4.2	157
TiO_2:LiOH	1:0.75	1.57	14.2	80.3	890.6	4.8	168

Based on Table 3, there was no catalytic reaction observed for TiO_2, and it is most likely due to the lower basicity of catalyst. Later the activity of the catalyst increased with a rise in the loading amount of Lithium ions up to an optimum value, beyond which reduction in the catalytic activity was detected probably due to a drop in both surface area and basicity [2,8,10,18]. Significant conversion of WCO to biodiesel was observed with TiO_2-0.5Li. Table 1 also shows the density, viscosity, and flash point of the obtained biodiesel were within the EN ISO 12185, EN ISO 3104, and EN ISO 2719 limits respectively [9,10,19].

2.3. Characterization of FAME

The composition of the biodiesel achieved by transesterification of WCO using the best catalyst, TiO_2-0.5Li, is shown in Figure 5. The FAME profile of the current sample was recognized with the support of the National Institute of Standards and Technology (NIST) 2014 Mass spectral (MS) library and described in Table 4.

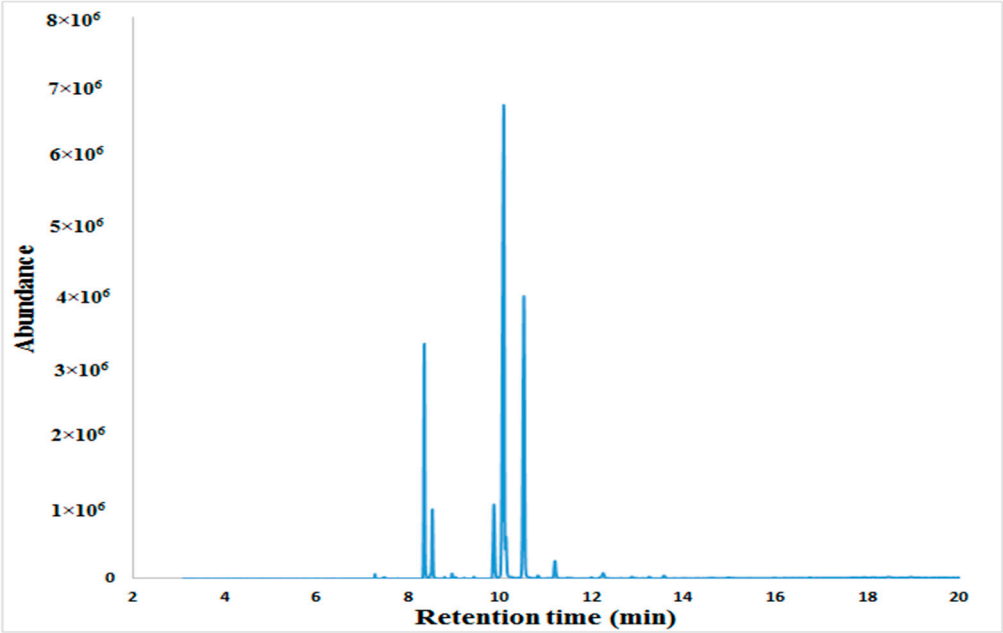

Figure 5. Illustrates the gas chromatography with mass spectrometry (GC-MS) spectrum of biodiesel obtained after transesterification with TiO_2-0.5Li.

Table 4. The biodiesel profile attained after transesterification with TiO_2-0.5Li.

Peak	Retention Time (min)	Library Match (%)	Compound Details
1	7.39	92	12-Methyltridecanoic acid methyl ester
2	8.34	91.7	Hexadecenoic acid, methyl ester
3	8.51	94.86	9-Hexadecenoic acid, methyl ester
4	9.86	94	Methyl stearate
5	10.1	96	13-Octadecenoic acid, methyl ester
6	10.5	96.48	11,14-Octadecadienoic acid, methyl ester
7	11.2	90	9,12,12-Octadecatrienoic acid, methyl ester
8	12.25	89.32	Myristic acid methyl ester

The percentage conversion of WCO to FAME and biodiesel characterization were estimated using ^{1}H and ^{13}C NMR spectroscopic methods, respectively. Figure 6a,b represents the ^{1}H and ^{13}C NMR spectra of the sample achieved after the transesterification of WCO using the TiO_2-0.5Li catalyst. The NMR spectra provided data that confirmed the presence of FAME. The 92.1% conversion of WCO to FAME was calculated with Equation (1) using the outcomes from ^{1}H NMR analysis.

The methoxy group (A_{ME}) of FAME and the methylene group (A_{CH2}) were well-defined by signals at 3.64 ppm and 2.28 ppm in the ^{1}H NMR spectra. Moreover, these signals also corresponded to the confirmation of methyl ester in the biodiesel sample. Besides signals used for calculation of FAME conversion percentage, there were other signals like 0.84 to 0.98 ppm for the latter methyl group. The existence of the methylene group and olefinic groups were confirmed by the signal in the range of 1.23 to 2.3 and at 5.3 ppm, respectively [2,10,16,18,20]. The existence of ester carbonyl –COO– and C–O were verified by signals at the range of 174 ppm and 51 ppm in ^{13}C NMR, correspondingly. The unsaturation in FAME samples was indicated by signals at 131.9 ppm and 127.1 ppm. The signals in the region of 20–34 ppm support the presence of $–CH_2$ group. Apart from these signals, the presence of terminal –CH3 groups was substantiated by signals at 14.1 and 14.2 ppm [2,15,20].

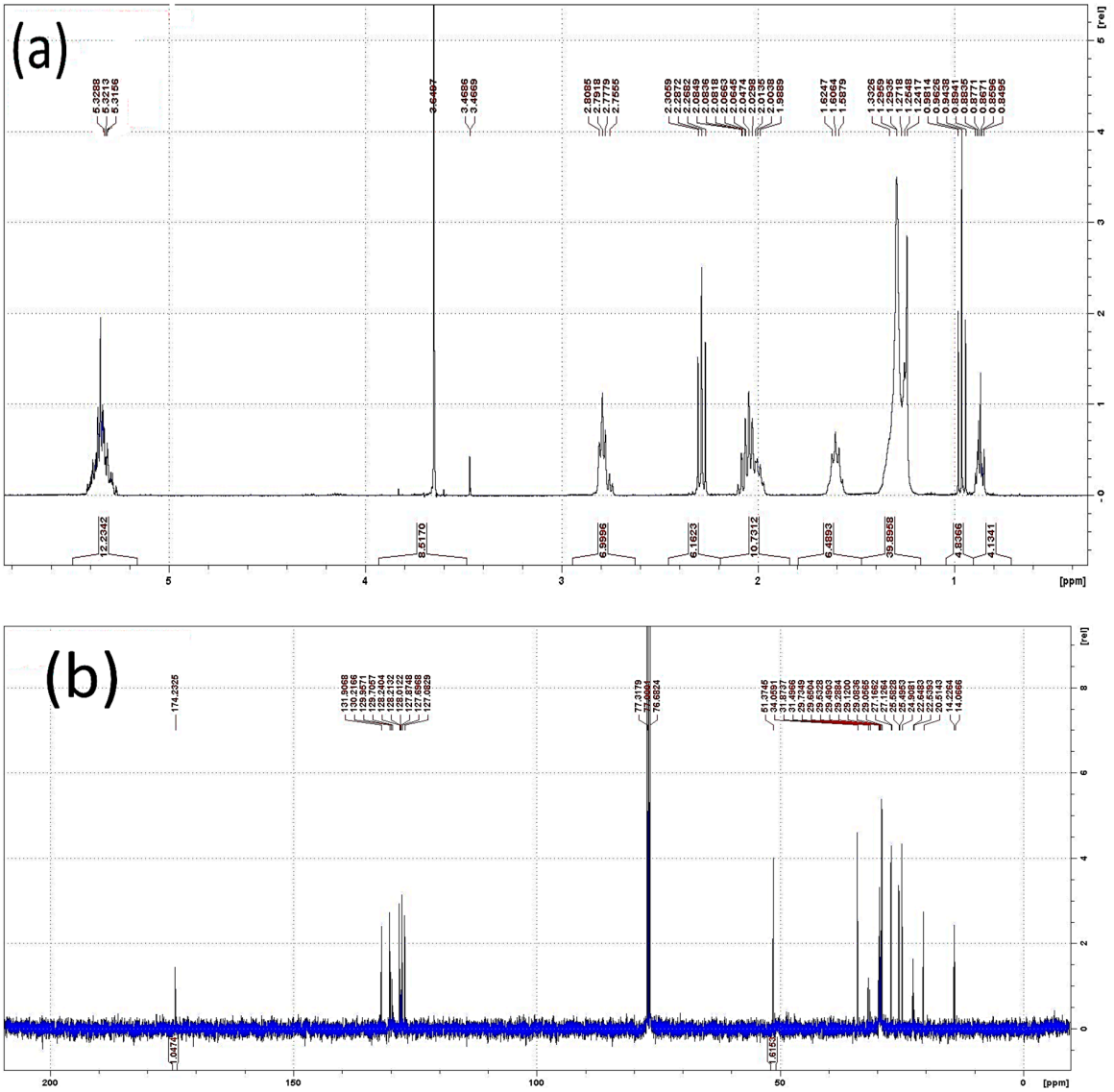

Figure 6. (**a**). The ^{1}H NMR for the biodiesel sample obtained with TiO_2-0.5Li (**b**). The ^{13}C NMR for the biodiesel sample obtained with TiO_2-0.5Li.

2.4. *Efficiency of REEs Removal*

The adsorption studies were performed using various nanomaterials such as TiO_2, TiO_2-LiOH (1:0.25, 1:0.5, and 1:0.75 molar ratios), and 50 mg/L of each REE solution with continuous mixing of samples at 250 rpm at 25 °C for 120 min. The adsorption capacity of different nanomaterials is illustrated in Figure 7. All nanomaterials showed adsorption efficiency of REEs, and the maximum adsorption capacity of nanomaterials was in the following order: TiO_2-0.5Li > TiO_2-0.75Li > TiO_2-0.25Li > TiO_2-0.5Li. The maximum adsorption of REEs was observed by TiO_2-0.5Li, probably due to the monoclinic crystal lattice and high basic strength of the catalyst [9,21–23].

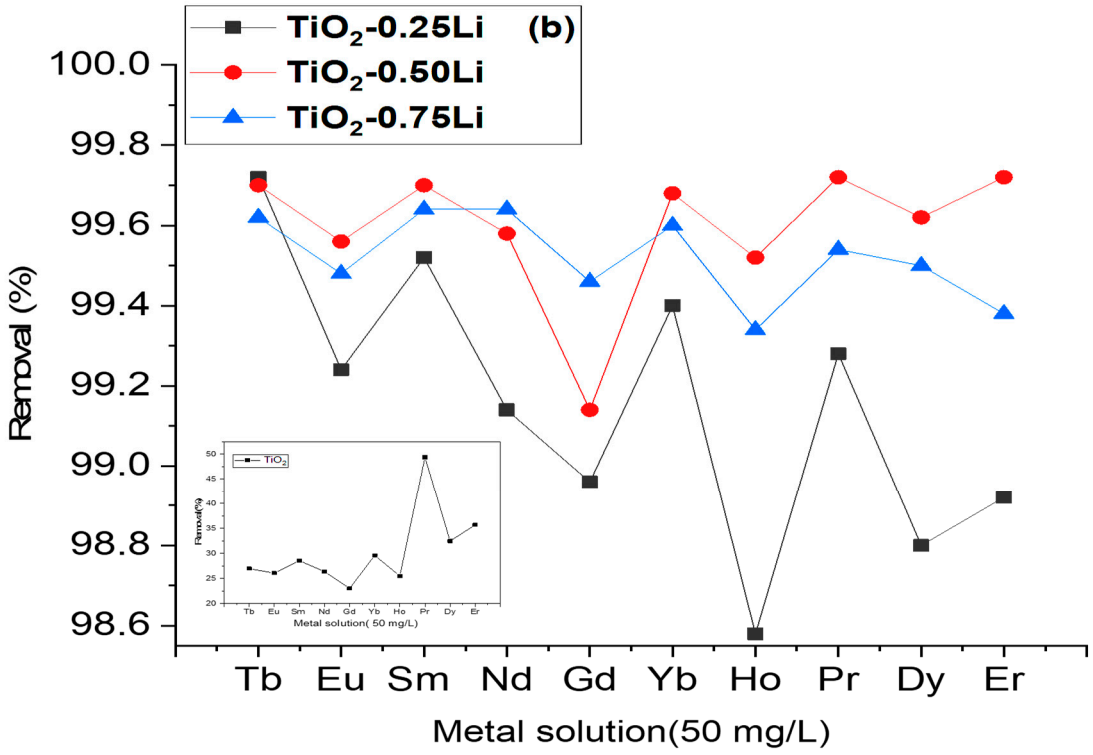

Figure 7. The adsorption efficiency of rare earth elements (REEs) using different nanomaterials.

3. Experimental

3.1. Materials

The REEs used in the present work include terbium (Tb^{3+}), europium (Eu^{3+}), samarium (Sm^{3+}), neodymium (Nd^{3+}), gadolinium (Gd^{3+}), ytterbium (Yb^{3+}), holmium (Ho^{3+}), praseodymium (Pr^{3+}), dysprosium (Dy^{3+}), and erbium (Er^{3+}). Waste cooking oil (FFA% = 0.754) was obtained from household waste, titanium oxide nanopowder (TiO_2), methanol (≥99.8%), and lithium hydroxide (LiOH) were purchased from Sigma-Aldrich (Espoo, Finland). All the chemicals were of analytical grade.

3.2. Catalyst Synthesis

The modification of TiO_2 by lithium-ions (Li+) was executed by the incipient wetness impregnation method. The preparation of catalysts was done by mixing TiO_2 and LiOH in different molar ratios of 1:0.25, 1:0.5, and 1:0.75. The TiO_2-LiOH solutions (i.e., 1 M TiO_2 solution mixed with 0.25 M, 0.5 M, 0.75 M LiOH solution, respectively) were constantly agitated for seven hours and followed by drying at 50 °C for 12 hours. The catalyst samples were calcined in a Naberthermb180 muffle furnace at 400 °C for four hours at 5 °C/min as the ramp rate of the temperature [8]. The catalyst samples were then denoted as TiO_2-xLi, where x represents the molar ratio. The conversion of WCO using TiO_2 and different concentrations of lithium-doped TiO_2 was conducted to select the best catalyst for biodiesel production.

3.3. Catalyst Characterization

The XRD patterns of TiO_2 and lithium-modified TiO_2 were performed using an X-ray diffractometer (XRD, PANalytical-Empyrean, Almelo, Netherlands) over a 2θ range of 10–120° with Co–Kα of 0.178 nm as an X-ray source at 40 mA and 40 kV. The scanning of bare TiO_2 and lithium-modified TiO_2 was executed by a scanning electron microscope (SEM, Hitachi SU3500, Tokyo, Japan) with a 5 kV accelerating voltage. The particle size of the catalysts was examined using a transmission electron microscope (TEM, Hitachi HT7700, Tokyo, Japan). The surface area of nanocatalyst samples was

done by Brunauer, Emmett, and Teller (BET, Micromeritics Tristar II plus, Norcross, USA). The basic strength of TiO_2 and lithium-modified TiO_2 was inspected using the Hammett indicator–benzene carboxylic acid titration method. The titration method conducted using the Hammett indicator–benzene carboxylic acid in which Hammett indicators like bromothymol blue (H_7.2), phenolphthalein (H_9.8), 2,4-dinitroaniline (H_15), and 4-nitroaniline (H_18.4) were used [2,8,10].

3.4. Biodiesel Production

The conversion of WCO to biodiesel using various catalysts was carried out by blending oil to methanol in a 1:6 molar ratio with 3 wt% of each nanocatalyst. The selection of the best catalyst for biodiesel production was performed by conducting the transesterification reaction experiments in triplicates in a 250 ml three-neck round-bottom flask with a reflux condenser and motorized stirrer at 65 °C for 120 min. The supernatant was collected when the phase separation of the samples was attained by the centrifugation of the reaction mixture. The recovery of nanocatalysts and additional methanol in the ester phase were achieved by centrifugation and rotary evaporator, respectively. The obtained supernatant was subjected to GC-MS analysis. The Agilent GC-MS (GC6890N, MS 5975) with the DB-wax FAME column (30 m, 0.25 mm, 0.25 µm) was used for the analysis of FAME containing supernatant. The analysis was performed in split mode with 250 °C as the inlet temperature. The oven temperature was programmed at 50 °C for 1 min and was raised at the rate of 25 °C/min to 200 °C and 3 °C/min to 230 °C and then it was held for 23 min. Esters of WCO after the transesterification reaction were investigated by ^1H and ^{13}C NMR (Bruker). The FAME analysis was performed by ^1H NMR and ^{13}C NMR at 400 MHz with $CDCl_3$ as a solvent. The conversion percentage of WCO to fatty acid methyl esters (C%) is estimated by Equation (1) [2,8,10,15].

$$C(\%) = \frac{2 \times Intergration\ value\ of\ protons\ of\ methyl\ ester}{3 \times Intergraton\ value\ of\ methyl\ protons} \times 100 \quad (1)$$

3.5. REEs Removal

REEs removal efficiency using synthesized nanomaterials was investigated by conducting adsorption experiments in batch mode. The metal solution of initial concentration 50 mg/L of Tb^{3+}, Eu^{3+}, Sm^{3+}, Nd^{3+}, Gd^{3+}, Yb^{3+}, Ho^{3+}, Pr^{3+}, Dy^{3+}, and Er^{3+} salts was prepared by dissolving the appropriate amount of each salt in deionized water. All the experiments were performed using 10 mL of corresponding REE metal solution and 30 mg of respective nanomaterial in a 15 mL centrifugation tube. The tube containing the catalyst and metal solution was placed in an IKA orbital shaker (KS 4000 ic control, Staufen, Germany) at a constant speed of 250 rpm for 120 min at 25 °C. The reaction mixture was filtered using 0.45 µm PTFE filters (Helsinki, Finland) from VWR and analyzed the concentrations of REEs by ICP-OES (Agilent, 5110).

4. Conclusions

The conversion of WCO to biodiesel and adsorption of REEs was efficiently performed using lithium-doped TiO_2. The effect of lithium concentration on the catalytic performance of TiO_2 was investigated, and the characterization of all prepared catalysts was done. The TiO_2-0.5Li nanocatalyst showed 92.1% conversion of WCO to fatty acid methyl ester and 99.7% recovery of REEs. The synthesized biodiesel properties were within the EN 14214 limits. Therefore, TiO_2-0.5Li (1:0.5 molar ratio) served as a multifunctional catalyst that showed great potential in the conversion of low-cost feedstock to biodiesel and REEs recovery.

Author Contributions: I.A. is the principal author and investigator, who planned, performed all experiments, analyzed all data, interpreted results, and wrote the first draft of the manuscript. E.H. helped with NMR data collection. V.S. and M.S. helped in the final drafting of the article and critical revision of the manuscript. All the authors gave their final approval for the submitted article.

Funding: There is no external funding for this research work.

Conflicts of Interest: The authors declare that they have no conflict of interest.

References

1. Ambat, I.; Srivastava, V.; Sillanpää, M. Recent advancement in biodiesel production methodologies using various feedstock: A review. *Renew. Sustain. Energy Rev.* **2018**, *90*, 356–369. [CrossRef]
2. Ambat, I.; Srivastava, V.; Haapaniemi, E.; Sillanpää, M. Application of Potassium Ion Impregnated Titanium Dioxide as Nanocatalyst for Transesterification of Linseed Oil. *Energy Fuels* **2018**, *32*, 11645–11655. [CrossRef]
3. Iftekhar, S.; Srivastava, V.; Sillanpää, M. Synthesis and Application of LDH Intercalated Cellulose Nanocomposite for Separation of Rare Earth Elements (REEs). *Chem. Eng. J.* **2016**, *309*, 130–139. [CrossRef]
4. Lakshmi, D.; Khan, S.; Repo, E.; Sillanpää, M. Synthesis of mesoporous and microporous amine and non-amine functionalized silica gels for the application of rare earth elements (REE) recovery from the waste water-understanding the role of pH, temperature, calcination and mechanism in Light REE and Heavy REE separation. *Chem. Eng. J.* **2017**, *322*, 56–65.
5. Srivastava, V.; Iftekhar, S.; Wang, Z.; Babu, I. Synthesis and application of biocompatible nontoxic nanoparticles for reclamation of Ce 3 þ from synthetic wastewater: Toxicity assessment, kinetic, isotherm and thermodynamic study. *J. Rare Earths* **2018**, *36*, 994–1006. [CrossRef]
6. Iftekhar, S.; Srivastava, V.; Ben, S.; Sillanpää, M. Fabrication of novel metal ion imprinted xanthan gum-layered double hydroxide nanocomposite for adsorption of rare earth elements. *Carbohydr. Polym.* **2018**, *194*, 274–284. [CrossRef]
7. Shi, W.; Li, J.; He, B.; Yan, F.; Cui, Z.; Wu, K.; Lin, L.; Qian, X.; Cheng, Y. Biodiesel production from waste chicken fat with low free fatty acids by an integrated catalytic process of composite membrane and sodium methoxide. *Bioresour. Technol.* **2013**, *139*, 316–322. [CrossRef]
8. Ambat, I.; Srivastava, V.; Haapaniemi, E.; Sillanpää, M. Effect of lithium ions on the catalytic efficiency of calcium oxide as a nanocatalyst for the transesterification of lard oil. *Sustain. Energy Fuels* **2019**, *3*, 2464–2474. [CrossRef]
9. Ambat, I.; Srivastava, V.; Iftekhar, S.; Haapaniemi, E.; Sillanpää, M. Dual application of divalent ion anchored catalyst: Biodiesel synthesis and photocatalytic degradation of carbamazepine. *Catal. Green Chem. Eng.* **2019**, *2*, 25–42. [CrossRef]
10. Ambat, I.; Srivastava, V.; Haapaniemi, E.; Sillanpää, M. Nano-magnetic potassium impregnated ceria as catalyst for the biodiesel production. *Renew. Energy* **2019**, *139*, 1428–1436. [CrossRef]
11. Rahman, M.L.; Biswas, T.K.; Sarkar, S.M. Adsorption of rare earth metals from water using a kenaf cellulose-based poly(hydroxamic acid) ligand—Elsevier Enhanced Reader. *J. Mol. Liq.* **2017**, *243*, 616–923. [CrossRef]
12. Iftekhar, S.; Srivastava, V.; Casas, A. Synthesis of novel GA-g-PAM/SiO_2 nanocomposite for the recovery of rare earth elements (REE) ions from aqueous solution. *J. Clean. Prod.* **2018**, *170*, 251–259. [CrossRef]
13. Ramasamy, D.L.; Wojtuś, A.; Repo, E.; Kalliola, S.; Srivastava, V.; Sillanpää, M. Ligand immobilized novel hybrid adsorbents for rare earth elements (REE) removal from waste water—Assessing the feasibility of using APTES functionalized silica in the hybridization process with chitosan. *Chem. Eng. J.* **2017**, *330*, 1370–1379. [CrossRef]
14. Anastopoulos, I.; Bhatnagar, A.; Lima, E.C. Adsorption of Rare Earth Metals: A review of recent literature Adsorption of rare earth metals: A review of recent literature. *J. Mol. Liq.* **2016**, *221*, 954–962. [CrossRef]
15. Ambat, I.; Srivastava, V.; Iftekhar, S.; Haapaniemi, E.; Sillanpää, M. Effect of different co-solvents on biodiesel production from various low-cost feedstocks using Sr-Al double oxides. *Renew. Energy* **2020**, *146*, 2158–2169. [CrossRef]
16. Singh, V.; Bux, F.; Sharma, Y.C. A low cost one pot synthesis of biodiesel from waste frying oil (WFO) using a novel material, β-potassium dizirconate (β-K2Zr2O5). *Appl. Energy* **2016**, *172*, 23–33. [CrossRef]
17. Boro, J.; Konwar, L.J.; Deka, D. Transesteri fi cation of non edible feedstock with lithium incorporated egg shell derived CaO for biodiesel production. *Fuel Process. Technol.* **2014**, *122*, 72–78. [CrossRef]
18. Qiu, F.; Li, Y.; Yang, D.; Li, X.; Sun, P. Bioresource Technology Heterogeneous solid base nanocatalyst: Preparation, characterization and application in biodiesel production. *Bioresour. Technol.* **2011**, *102*, 4150–4156. [CrossRef]

19. Singh, S.P.; Singh, D. Biodiesel production through the use of different sources and characterization of oils and their esters as the substitute of diesel: A review. *Renew. Sustain. Energy Rev.* **2010**, *14*, 200–216. [CrossRef]
20. Tariq, M.; Ali, S.; Khalid, N. Activity of homogeneous and heterogeneous catalysts, spectroscopic and chromatographic characterization of biodiesel: A review. *Renew. Sustain. Energy Rev.* **2012**, *16*, 6303–6316. [CrossRef]
21. Basahel, S.N.; Ali, T.T.; Mokhtar, M.; Narasimharao, K. Influence of crystal structure of nanosized ZrO_2 on photocatalytic degradation of methyl orange. *Nanoscale Res. Lett.* **2015**, *10*, 73. [CrossRef] [PubMed]
22. Ben, S.; Zhao, F.; Safaei, Z.; Babu, I.; Lakshmi, D.; Sillanpää, M. Reactivity of novel Ceria–Perovskite composites CeO2-LaMO3 (MCu, Fe) in the catalytic wet peroxidative oxidation of the new emergent pollutant 'Bisphenol F': Characterization, kinetic and mechanism studies. *Appl. Catal. B Environ.* **2017**, *218*, 119–136.
23. Pourret, O.; Houben, D. Characterization of metal binding sites onto biochar using rare earth elements as a fingerprint. *Heliyon* **2018**, *4*, e00543. [CrossRef] [PubMed]